MIMO Smith Predictor: Global and Structured Robust Performance Analysis ⋆

Ricardo S. Sánchez-Peña [b,*], Yolanda Bolea and Vicenç Puig

Sistemas Avanzados de Control
Universitat Politècnica de Catalunya (UPC)
ESAII, Terrassa, Barcelona, Spain

[b] *Institució Catalana de Recerca i Estudis Avançats, Barcelona, Spain*

Abstract

The purpose of this work is to extend the analysis of the Smith predictor structure to multiple-input multiple-output (MIMO) systems with uncertain multiple delays. This is applied to the set of models that can be factorized into a rational MIMO model in series with left/right diagonal (multiple) delay matrices. Necessary and sufficient conditions on the plant's model to achieve this factorization are proved. This factorized structure is instrumental for the structured robustness analysis and applies to multiple pool open flow canals. Nominal and robust performance and stability are analyzed for the case of plants with multiple uncertain delays for two different uncertainty structures: global dynamic and structured parametric. The first uncertainty structure could also accommodate the dynamic uncertainty of the plant's rational part as well. This analysis is applied to a controller designed for a two-pool canal system.

Key words: Smith Predictor, robust performance, dynamic uncertainty, parametric uncertainty, multiple uncertain delays.

⋆ This research was supported by the Research Commission of the *Generalitat de Catalunya* (ref. 2005SGR00537), and by the Spanish CICYT (ref. DPI2005-04722).

* Corresponding author.

[1] *Email addresses*: {ricardo.sanchez-pena/yolanda.bolea/vicenc.puig}@upc.edu

1 Introduction

Time delay is a fundamental characteristic of many multivariable processes in practice. Multiple time delays existing in individual loops tend to deteriorate decoupling regulation. A well known control scheme for time-delay systems is the *Smith predictor*. It is based on introducing a compensation loop inside the controller with the purpose of cancelling the effect of the dead time on the dynamics of the closed loop. This facilitates the tuning of the controller and permits analyzing stability using conventional methods. This approach has been used extensively since the time it was first proposed in [1], and is now an established and effective control scheme (see also a tutorial in [2]). One of the main properties of this approach is that the transfer function of the controlled system can be factored into a product of a delay free system and a pure time-delay. There have been several partially successful attempts to generalize the Smith predictor for the control of MIMO systems, all using the structure in Figure 1. In [3,4], it was assumed that all delays in each input-output channel were equal. In [5] a delay is associated with each sensor, i.e. equal delays in each row of the plant. One of the major works in this area are [6–9], which generalize the results in [1,3,5] to delays in all system elements. The analysis in all previous works is centered around the nominal internal stability of the closed loop. Ogunnaike's work ([6]), unlike the single-input single-output (SISO) Smith controller, fails to achieve the desired output performance expected from the delay-free design because the delays in the process could mix up the outputs of the delay-free part. Thus, the performance of this MIMO Smith controller might be poor, as indicated in [10].

An improvement over [6] is presented in [11], where not only stability but also performance is introduced, basically as set-point changes, which in this case also generalize the SISO result. Furthermore, three properties of the Smith predictor are introduced, which are useful for classifying the effectiveness of further generalizations of this control structure. In particular, the third property is the factorization of the system into a product of a delay free and a pure time-delay model, as mentioned before. In this case, the pure delay model is a left (or possibly right) full MIMO system. In addition, performance improvements can be reached in some cases *via* the addition of delays in some of the I/O channels. Other results that use decoupling techniques have been presented in [12,13], further extended in [14]. The delayed model is converted to a diagonal delayed form, which is a particular case of the result in [5]. The focus in these works is to produce simple PID controllers rather than to obtain the best possible performance.

Previous results deal mainly with nominal stability or performance. The first re-

sult that analyzes robust (internal) stability under global additive uncertainty as instances of Internal Model Control (IMC) ([10]), is presented in [15]. The solution is simpler than the ones presented in [8,9,16], generalizes [6,7], and allows studying stability robustness following the approach proposed by [17], extended to the MIMO case. A similar evaluation of global dynamic uncertainty which includes altogether model and delay uncertainty can be found in [13]. There the plant decoupling applies only to the nominal case, but fails in the uncertain case where robustness needs to be evaluated globally. There are yet no results that deal with structured uncertainty neither for stability nor performance.

The previous comments agree with a usual criticism of the Smith predictor: controllers with this structure can be very sensitive to modelling errors, particularly in the time delays. It is shown in [18], that the Smith predictor controller could produce an unstable loop for an infinitesimal perturbation in the dead time, even though it may be nominally stable. Therefore robust stability for multiple delay uncertainty in MIMO systems is another problem to be solved in this area of research.

Finally, a synthesis result to achieve nominal performance has been presented in [19] with an $\mathcal{H}_\infty$ criteria. The optimal $\mathcal{H}_\infty$ controller designed is a rational MIMO system (which could have solved optimal robust stability under global dynamic uncertainty as well). A left/right factorization of the original plant has been considered, where the left/right pure delay models are diagonal and the central model is delay-free: the same structure we have presented here (see equation (2)). The authors do not provide the class of plants that can be factorized in this way and, in addition, consider that *...there appears to be no natural generalization of single-delay Smith predictor schemes to the case of multiple delays...* and suggest that, along the lines of their work, a possible generalization could be made.

To recap, from a general point of view, Smith Predictors are based on separating the infinite dimensional dynamics (delays) from the finite dimensional ones (rational model). In the MIMO case a general factorization would be a left/right multiple delay matrices in series with a rational one, as in [6] and [11]. The original contribution of the Smith Predictor ([1]) was intended for the nominal case, i.e. no uncertainty. In that case, "full" delay matrices can be taken into consideration and used effectively to improve performance. Nevertheless, when uncertainty is considered, the general factorization with "full" delay matrices complicates the analysis. In this case (as in [6,11]) there is not yet a tool that provides precise robustness margins for stability and/or performance. An alternative is to "cover" with global dynamic uncertainty the delay uncertainty (as in [13,15] or as we do in our first approach) at the expense of conservative results in general. A better alternative at this point is to restrict the set of models to the ones that may achieve this factoriza-

tion but for diagonal multiple delay matrices, as suggested in [19]. In our work we adopt this factorization structure, and surprisingly these plants are not as artificial as could be assumed: multiple pool open flow canal systems meet the factorization conditions.

Hence, from an analysis standpoint, a left/right factorization seems more reasonable when considering a MIMO system and the diagonal delayed models can be used for robustness analysis. The purpose of this work is to extend the analysis of the Smith predictor structure in [6] to MIMO systems with multiple delay uncertainty. First, we present necessary and sufficient conditions on the plant's model to have a diagonal left/right factorization (the *third property* in [11]), which applies to multiple pool open flow canals. Next, nominal and robust performance and stability are analyzed for the case of plants with multiple uncertain delays for two different uncertainty structures: global dynamic and structured parametric. The first uncertainty structure could also accommodate the dynamic uncertainty of the plant's rational part, as well. In addition, performance is defined either as disturbance rejection (DR) or tracking error (TE) for *sets* of disturbance/reference signals, which seems more practical than previous definitions which consider a *single* known disturbance/reference (usually set-point changes). Finally, this analysis is applied to a two-pool canal system and compared to previous methods. This analysis procedure generalizes for multiple delay MIMO models, the IMC analysis of the Smith predictor in [17], also developed in chapter 11.2 of [20]).

The paper is organized as follows. Next section presents the general conditions which should be met to separate a MIMO model with multiple delays into its rational and pure delay (left and right) matrices. In section 3, uncertainty in the multiple delays is considered in two cases: global (dynamic) and structured (parametric), and the corresponding robust stability equivalent conditions are derived. Section 4 defines performance in the Tracking error and Disturbance rejection cases, and computes nominal and robust equivalent conditions. All previous results are applied in section 5 to a two-pool canal system and a controller is designed by using the Youla parametrization. Robust stability and performance are evaluated for structured and unstructured uncertainty. Another example in section 6 compares the analysis methodology presented here with previous methods, particularly in terms of robustness, performance and decoupling. Final conclusions and research directions end this work in section 7.

2 General model decomposition

The purpose of this section is to provide necessary and sufficient conditions to define the class of plants that can be factorized as diagonal left/right delays and a rational model (the *third property* in [11]). This is instrumental in extending the robustness analysis of Smith predictors to MIMO systems with multiple uncertain delays. This decomposition has already been used in a synthesis framework ([19]). The uncertainty model can be considered either as global dynamic or structured parametric, as will be shown in sections 3 and 4. Furthermore, uncertainty in the rational part of the system may also be accommodated under this same scheme.

Consider the model:

$$G(s) = [g_{ij}(s)e^{s\tau_{ij}}], \qquad i = 1, \ldots, n \; ; \; j = 1, \ldots, m \tag{1}$$

for which we seek the following decomposition (see [19]):

$$G(s) = \left[g_{ij}(s)e^{-s\tau_{ij}}\right] = \text{ diag}\left[e^{-s\tau_i^\ell}\right] G_m(s) \text{ diag}\left[e^{-s\tau_j^r}\right] \tag{2}$$

$$G_m(s) = [g_{ij}(s)], \qquad i = 1, \ldots, n \; ; \; j = 1, \ldots, m \tag{3}$$

To find these left (τ_i^ℓ) and right delays (τ_i^r), we need to solve the following linear equation:

$$\begin{bmatrix} \tau_{11} \\ \vdots \\ \tau_{n1} \\ \tau_{12} \\ \vdots \\ \tau_{nm} \end{bmatrix} = \begin{bmatrix} I_n & \mathbf{1}_n & & & \mathbf{0}_{n\times(m-1)} \\ I_n & \mathbf{0}_n & \mathbf{1}_n & & \mathbf{0}_{n\times(m-2)} \\ \vdots & \vdots & \vdots & & \vdots \\ I_n & & \mathbf{0}_{n\times(m-1)} & & \mathbf{1}_n \end{bmatrix} \begin{bmatrix} \tau_1^\ell \\ \vdots \\ \tau_n^\ell \\ \tau_1^r \\ \vdots \\ \tau_m^r \end{bmatrix} \triangleq H\tau \tag{4}$$

with $H \in \mathbb{R}^{nm\times(n+m)}$, and $\mathbf{1}_n$ ($\mathbf{0}_n$) a column vector of ones (zeros) of length n. This linear equation has a solution in the following conditions.

Lemma 2.1 *The rank of the previous matrix is $r \leq (n + m - 1)$ and, in general, there is a solution only for SIMO, MISO*[2] *or diagonal systems.*

[2] Single Input Multiple Output, and Multiple Input Single Output

Proof: See Appendix A.

This is the case of the example found in [21]. Other works in this area diagonalize the model so that SISO techniques can be applied (see for example [12,22]). Here we seek a solution to these equations without transforming the whole plant to a diagonal model, but instead finding the functional relations between delays so that a factorization between rational and delayed portions of the model can be made. The main result follows.

Lemma 2.2 *For MIMO systems in general, there exists a solution to the previous linear equation if and only if the following relations hold:*

$$\tau_{i,q} - \tau_{j,q} = \tau_{i,k} - \tau_{j,k}, \quad \begin{cases} i = 1, \ldots, n & j = 1, \ldots, n \\ q = 1, \ldots, m & k = 1, \ldots, m \end{cases} \tag{5}$$

Proof: See Appendix B.

This seems an artificial condition, but surprisingly, it is satisfied by multiple pool open flow canals [3], as will be presented in the application example of section 5. For particular system structures, less restrictive conditions can be stated, as will be proved next.

Corollary 2.1 *In the case of lower (upper) triangular systems, there exists a solution to the previous linear equation (4) only for systems with dimension $n \leq 2$. For a general lower (upper) triangular system, there is a solution if and only if the following relations hold:*

$$\tau_{i,q} - \tau_{j,q} = \tau_{i,k} - \tau_{j,k}, \quad \begin{cases} i = 1, \ldots, n & j = 1, \ldots, n \\ i \geq q, k & j \geq q, k \end{cases}$$

Proof: See Appendix C.

[3] Note also that in [11], additional delays are applied to certain channels to improve performance. Here the same procedure could be applied in order to force the conditions (5) to be met in a general case so that a left/right diagonal decomposition could be made (see example in section 6).

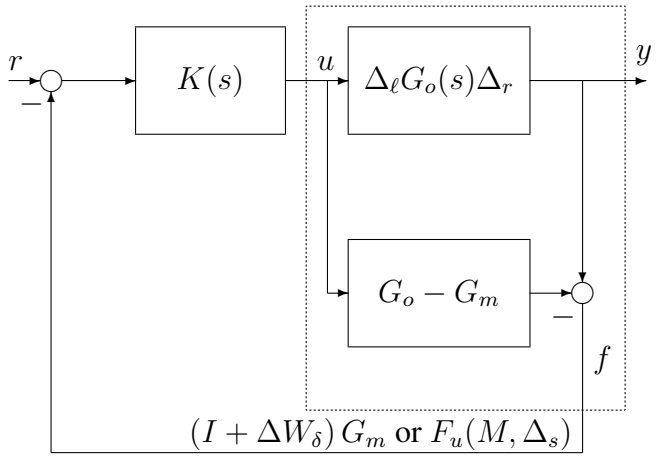

Fig. 1. Smith Predictor with uncertainty: global or structured.

3 Robust Stability

Once the factorization of the plant's model which separates delays from rational part has been made, the delay uncertainty is considered. The uncertain model of the plant is:

$$
\begin{aligned}
G(s) &= D_\ell(s) G_m(s) D_r(s) = \Delta_\ell(s) G_o(s) \Delta_r(s), \\
D_\ell(s) &= \text{ diag } \left[e^{-s\tau_i} \right] = \Delta_\ell \bar{D}_\ell(s) \stackrel{\triangle}{=} \text{ diag } \left[e^{-s\delta_i} \right] \cdot \text{ diag } \left[e^{-s\bar{\tau}_i} \right], \; i = 1, \ldots, n \\
D_r(s) &= \text{ diag } \left[e^{-s\tau_j} \right] = \Delta_r \bar{D}_r(s) \stackrel{\triangle}{=} \text{ diag } \left[e^{-s\delta_j} \right] \cdot \text{ diag } \left[e^{-s\bar{\tau}_j} \right], \; j = 1, \ldots, m \\
G_o(s) &\stackrel{\triangle}{=} \bar{D}_\ell(s) G_m(s) \bar{D}_r(s)
\end{aligned}
$$

Due to its diagonal structure, uncertainty and nominal delay are commutative, i.e $\Delta_{\ell(r)} \bar{D}_{\ell(r)} = \bar{D}_{\ell(r)} \Delta_{\ell(r)}$. Here, the nominal (delayed) model has been defined as $G_o(s)$ and the rational (delay-free) part as $G_m(s)$.

The uncertain model is obtained from the Smith Predictor structure (figure 1), between input u and the feedback output f:

$$
[G_m(s) + G(s) - G_o(s)] = [\Delta_\ell(s) G_o(s) \Delta_r(s) - G_o(s) + G_m(s)] \tag{6}
$$

3.1 Global dynamic uncertainty

A simple way to include delay uncertainty in the set of models is to cover it completely with global uncertainty that does not distinguish between the different input/output channels. In this case we may put equation (6) in the following way:

$$\left[\Delta_\ell(s) \; -I\right] G_o(s) \begin{bmatrix} \Delta_r(s) \\ I \end{bmatrix} + G_m(s) \tag{7}$$

The following result applies.

Lemma 3.1 *The uncertainty in the delay can be covered by the following global dynamic uncertain set of models:*

$$\mathcal{G}(s) \stackrel{\triangle}{=} \{[I + \Delta W_\delta(s)]\, G_m(s), \quad \Delta \in \mathbb{C},\ \bar{\sigma}(\Delta) < 1\} \tag{8}$$

with $W_\delta(s) = w_\delta(s)I$, $w_\delta(s)$ a SISO stable non-minimum phase linear model such that $|w_\delta(\jmath\omega)| \geq 2\kappa\,[G_m(\jmath\omega)]$. Here $\kappa(\cdot)$ is the condition number and I the identity matrix of adequate dimensions.

Proof: See Appendix D.

Remarks:

- In the SISO case, presented in [17,23] or Chapter 11.2 in [20], $|w_\delta(\jmath\omega)|$ "covers" $|e^{-\jmath\omega\delta} - 1|$, where the latter depends on the parametric uncertainty interval $\delta \in [a, b]$. Therefore, the delay (parametric) uncertainty is covered by multiplicative dynamic uncertainty $[1 + w_\delta(s)\Delta]$. In the MIMO case, $\bar{\sigma}\left(\Delta_\ell G_m \Delta_r - G_m\right)$ is obtained from equation (6) after pulling out the nominal delays $\bar{D}_\ell$ and $\bar{D}_r$. Therefore the coverage of the left (right) matrix $\Delta_\ell - I$ ($\Delta_r - I$) cannot be obtained because left and right uncertainty matrices do not commute with $G_m(s)$ in general. Clearly it reduces to $|(e^{-\jmath\omega\delta} - 1)|$ in the SISO case, which can be covered as mentioned previously.
- The same conditions can be used to incorporate to the delay uncertainty, the dynamic uncertainty of model $G_m(s)$, by covering both uncertainties simultaneously with $W_\delta(s)$.
- For the set of models (8), robust stability is equivalent [4] to $\|W_\delta(s)T_m(s)\|_\infty < 1$,

[4] It is equivalent for the multiplicative dynamic uncertainty set (8), but not for the actual

where T_m is the complementary sensitivity function corresponding to model G_m (similarly we define the sensitivity S_m). Due to the fact that the condition number $\kappa(\cdot) \geq 1$, the uncertainty weight is overly conservative, and forces $\bar{\sigma}(T_m) \leq \frac{1}{2}$ at all frequencies. As a consequence it is convenient to obtain a less conservative weight. This can be done by using equation (D.1) to define W_δ, as will be applied in the example (left plot in Figure 5), or by exploiting the structure of the uncertainty, as will be presented in next subsection.

3.2 Structured parametric uncertainty

To take advantage of the uncertainty structure instead, we can transform equation (6) non conservatively as a set of models represented by a LFT [5], in a standard way. Here the uncertainty is not global, but has a particular structure represented by set $\mathbf{\Delta}_s$, as shown next.

$$\text{Eqn.}(6) = F_u\left[M(s), \Delta\right] = \left[\Delta_\ell(s) G_o(s) \Delta_r(s) - G_o(s) + G_m(s)\right]$$

$$M(s) = \begin{bmatrix} \mathbf{0}_{n\times n} & G_o & G_o \\ \mathbf{0}_{m\times n} & \mathbf{0}_{m\times m} & I_m \\ I_m & G_o & G_m \end{bmatrix}$$

$$\Delta \in \mathbf{\Delta_s} \triangleq \left\{ \begin{bmatrix} \Delta_\ell - I_n & \mathbf{0} \\ \mathbf{0} & \Delta_r - I_m \end{bmatrix} = \begin{bmatrix} e^{-s\delta_1} - 1 & \dots & \mathbf{0} \\ \vdots & \ddots & \vdots \\ \mathbf{0} & \dots & e^{-s\delta_{(n+m)}} - 1 \end{bmatrix}, \begin{array}{l} \delta_i \in [a_i, b_i] \\ \delta_i \in \mathbb{R} \end{array} \right\}$$

Matrix $M(s)$ can be obtained through simple manipulations from figure 1, or otherwise it can be verified that $F_u\left[M(s), \Delta\right]$ equals equation (6). Note that the phase uncertainty at each input/output channel separately, can also be covered by multiplicative uncertainty as in the SISO case (see Remarks after Lemma 3.1). To compute the stability margin for this type of uncertainty, we obtain the transfer matrix between u_δ and y_δ as follows:

---

delay uncertain family of models, for which it is only sufficient in case $W_\delta(s)$ performs an adequate "coverage" of the delay parametric uncertainty.

[5] Linear Fractional Transformation: $F_u(A, X) = A_{22} + A_{21} X \left(I - A_{11} X\right)^{-1} A_{12}$ and $F_\ell(A, Y) = A_{11} + A_{12} Y \left(I - A_{22} Y\right)^{-1} A_{21}$.

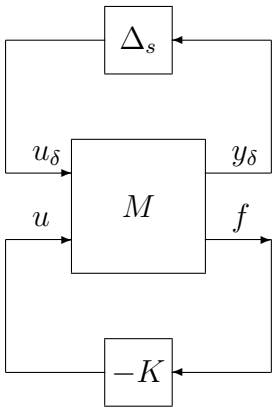

Fig. 2. Structured uncertainty analysis.

$$
\begin{aligned}
y_\delta(s) &= F_\ell\left[M(s), K(s)\right] u_\delta(s) \triangleq T(s) u_\delta(s) \\
T(s) &= \begin{bmatrix} \mathbf{0}_{n\times n} & G_o \\ \mathbf{0}_{m\times n} & \mathbf{0}_{m\times m} \end{bmatrix} + \begin{bmatrix} G_o \\ I_m \end{bmatrix} K\left(I + G_m K\right)^{-1} \begin{bmatrix} I_m & G_o \end{bmatrix} \\
&= - \begin{bmatrix} G_o(s)K(s)S_m(s) & \left[G_o(s)K(s)S_m(s) - I\right]G_o(s) \\ K(s)S_m(s) & K(s)S_m(s)G_o(s) \end{bmatrix}
\end{aligned} \tag{9}
$$

The exact stability margin should be computed as follows:

$$
k_{\mathbf{\Delta_s}}(\jmath\omega) = \left[\inf\left\{\max\|\Delta\| \text{ s.t. } \det\left[I - T(\jmath\omega)\Delta\right] = 0,\ \Delta \in \mathbf{\Delta_s}\right\}\right]^{-1}
$$

Hence, the uncertain system $\left\{F_u\left[T(s), \Delta_s\right],\ \Delta_s \in \mathcal{B}\mathbf{\Delta_s}\right\}$ is robustly stable if and only if $k_{\mathbf{\Delta_s}}(\jmath\omega) < 1$, for all ω, where $\mathcal{B}\mathbf{\Delta_s}$ represents the unit ball with structure $\mathbf{\Delta_s}$. The exact stability margin cannot be computed exactly with existing computational tools, but by covering the individual delay uncertainties with multiplicative dynamic SISO uncertainty, a (tight) upper bound can be found as follows:

$$
\begin{aligned}
& \left\{(e^{-s\delta_i} - 1),\ \delta_i \in [a_i, b_i]\right\} \subset \left\{1 + w_{\delta i}(s)\Delta_i,\ |\Delta_i| < 1\right\} \\
\Longrightarrow \quad & k_{\mathbf{\Delta_s}}(\jmath\omega) \leq \mu_{\mathbf{\Delta}}\left[W_\delta^s(\jmath\omega)T(\jmath\omega)\right] < 1, \quad W_\delta^s(s) = \text{ diag}[w_{\delta_i}] \\
\mathbf{\Delta} \triangleq & \left\{ \text{diag}\left[\Delta_1 \ \ldots \ \Delta_{(n+m)}\right], \quad \Delta_i \in \mathbb{C}\right\}
\end{aligned}
$$

where $\mu_{\mathbf{\Delta}}(\cdot)$ is the structured singular value computed with respect to the uncertainty structure $\mathbf{\Delta}$ ([24,23,20]). This value $\mu_{\mathbf{\Delta}}(\cdot)$ will be a tight upper bound on the actual stability margin, depending on how close the weight $w_{\delta i}(s)$ covers the

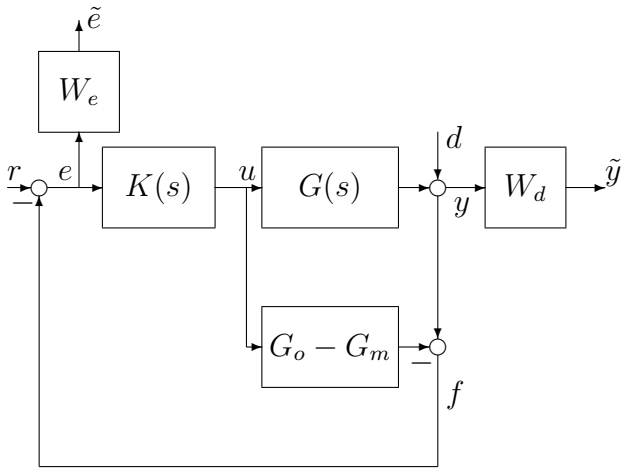

Fig. 3. Output disturbance rejection and tracking as performance measures.

magnitude of the delay uncertainty $\left|e^{-s\delta_i} - 1\right|$. Note that to use this analysis tool for controller synthesis is non trivial, because the matrix $T(s)$ contains a delayed (infinite dimensional) system $G_o(s)$.

4 Robust Performance

4.1 Nominal Performance

Two practical performance criteria will be considered: (output) disturbance rejection and tracking for *sets* of disturbance/reference signals. Therefore in Figure 3 we add a disturbance $d(s)$ at the plant's output to measure its effect at $y(s)$. This excitation signal can be weighted by a model $W_d(s)$ which, in general, could take into account the frequency distribution and relative magnitude of the perturbation and/or the output signal. We also add a weight $W_e(s)$ to measure the tracking error e due to a reference signal r. Both input and output signals are measured in terms of their energy, i.e. the 2–norm. Both performance criteria are as follows:

TE Tracking Error performance criteria:

$$\|W_e(s)e(s)\|_2 < 1, \quad \forall \|r(s)\|_2 \leq 1 \Longleftrightarrow \|W_e(s)T_{er}(s)\|_\infty < 1 \tag{10}$$

DR Disturbance Rejection performance criteria:

$$\|W_d(s)y(s)\|_2 < 1, \quad \forall \|d(s)\|_2 \leq 1 \Longleftrightarrow \|W_d(s)T_{yd}(s)\|_\infty < 1 \tag{11}$$

Here $T_{er}(s)$ and $T_{yd}(s)$ are the transfer matrices from $r \to e$ and $d \to y$, respectively. They can be obtained by simple manipulation of blocks from Figure 3:

$$
\begin{aligned}
T_{er}(s) &= \left[I + (G - G_o + G_m)\, K\right]^{-1} = \left[S_m^{-1} + (G - G_o)\, K\right]^{-1} \\
&= S_m \left[I + (G - G_o) K S_m\right]^{-1} \qquad (12) \\
T_{yd}(s) &= \left\{I + GK \left[I + (G_m - G_o)\, K\right]^{-1}\right\}^{-1} \\
&= \left[I + GK \left(S_m^{-1} - G_o K\right)^{-1}\right]^{-1} \\
&= (I - G_o K S_m) \left[I + (G - G_o)\, K S_m\right]^{-1} \qquad (13)
\end{aligned}
$$

For simplicity we have eliminated the dependency with variable s in all systems. The first term of last equation reduces to $[1 - e^{s\tau_o} T_m(s)]$ in the SISO case, as in the example of Chapter 11, equation (11.23) [20].

Applying the performance criteria in (10) and (11) to the nominal model ($G \equiv G_o$), the following nominal performance equivalent conditions are obtained:

TE Tracking Error $\Longleftrightarrow \bar{\sigma}\left\{W_e(s) S_m(s)\right\} \leq 1,\ \forall s = \jmath\omega$
DR Disturbance Rejection $\Longleftrightarrow \bar{\sigma}\left\{W_d(s)\left[I - G_o(s) K(s) S_m(s)\right]\right\} \leq 1,\ \forall s = \jmath\omega$

4.2 Robust performance: global uncertainty

Applying the same criteria in (10) and (11) to the globally uncertain set of models, the following robust performance sufficient conditions are obtained:

TE Tracking Error.

$$
\begin{aligned}
&\Longleftrightarrow \bar{\sigma}\left\{W_e S_m \left[I + \Delta W_\delta T_m\right]^{-1}\right\} \leq 1,\ \forall \|\Delta\| < 1, s = \jmath\omega \\
&\Longleftarrow \bar{\sigma}\left[W_e S_m\right] \leq \underline{\sigma}\left[I + \Delta W_\delta T_m\right],\ \forall \|\Delta\| < 1, s = \jmath\omega \\
&\Longleftarrow \bar{\sigma}\left[W_e S_m\right] + \bar{\sigma}\left[\Delta W_\delta T_m\right] \leq 1,\ \forall \|\Delta\| < 1, s = \jmath\omega \\
&\Longleftarrow \bar{\sigma}\left[W_e(s) S_m(s)\right] + \bar{\sigma}\left[W_\delta(s) T_m(s)\right] \leq 1,\ \forall s = \jmath\omega \qquad (14)
\end{aligned}
$$

DR Disturbance Rejection.

$$
\begin{aligned}
&\Longleftrightarrow \bar{\sigma}\left\{W_d \left[I + G_o K S_m\right] \left[I + \Delta W_\delta T_m\right]^{-1}\right\} \leq 1,\ \forall \|\Delta\| < 1, s = \jmath\omega \\
&\Longleftarrow \bar{\sigma}\left\{W_d \left[I + G_o K S_m\right]\right\} \leq \underline{\sigma}\left[I + \Delta W_\delta T_m\right],\ \forall \|\Delta\| < 1, s = \jmath\omega \\
&\Longleftarrow \bar{\sigma}\left\{W_d \left[I + G_o K S_m\right]\right\} + \bar{\sigma}\left[\Delta W_\delta T_m\right] \leq 1,\ \forall \|\Delta\| < 1, s = \jmath\omega \\
&\Longleftarrow \bar{\sigma}\left\{W_d \left[I + G_o(s) K(s) S_m(s)\right]\right\} + \bar{\sigma}\left[W_\delta(s) T_m(s)\right] \leq 1, \qquad (15) \\
&\qquad \forall s = \jmath\omega
\end{aligned}
$$

Note that the performance conditions for **TE** are simpler than the ones for **DR** due to the fact that the input and output signals in the former case (r, e) do not involve

the Smith Predictor loop. Furthermore, the robust performance condition for **TE** is independent of the nominal delays, due to the same fact.

4.3 Robust performance: structured uncertainty

Applying the same procedure as in the case of robust stability under delay (parametric) uncertainty, the transfer matrix between input and output signals $(r, \tilde{e})$ for TE and $(d, \tilde{y})$ for DR, respectively, are presented next.

$$\begin{bmatrix} y_\delta \\ \tilde{e} \end{bmatrix} = \underbrace{\begin{bmatrix} & T(s) & & G_o K S_m \\ & & & K S_m \\ -W_e S_m & -W_e S_m G_o & & W_e S_m \end{bmatrix}}_{T_{TE}(s)} \begin{bmatrix} u_\delta \\ r \end{bmatrix}$$

$$\begin{bmatrix} y_\delta \\ \tilde{y} \end{bmatrix} = \underbrace{\begin{bmatrix} & T(s) & & G_o K S_m \\ & & & K S_m \\ -W_d G_o K S_m & -W_d G_o K S_m G_o & & W_d \left[I - G_o K S_m \right] \end{bmatrix}}_{T_{DR}(s)} \begin{bmatrix} u_\delta \\ d \end{bmatrix}$$

Robust performance is therefore guaranteed if and only if:

$$\left\| F_u \left[T_p(s), \Delta \right] \right\|_\infty < 1 \quad \forall \Delta \in \mathbf{\Delta_s}$$

where $T(s)$ has been defined in (9) and $T_p(s)$ is alternatively $T_{TE}(s)$ or $T_{DR}(s)$ depending on the performance criteria. The exact value of the above equation cannot be computed exactly with existing computational tools, but using a similar coverage of the delay uncertainty by complex multiplicative uncertainty, a (tight) upper bound can be found as follows:

$$\begin{aligned} &\text{RP} \Longleftarrow \mu_{\mathbf{\Delta_p}} \left[W_\delta^p(\jmath\omega) T_p(\jmath\omega) \right] < 1, \quad \forall \omega \\ &\mathbf{\Delta_p} \triangleq \left\{ \begin{bmatrix} \Delta & \mathbf{0} \\ \mathbf{0} & \Delta_p \end{bmatrix}, \ \Delta \in \mathbf{\Delta}, \ \Delta_p \in \mathbb{C}^{r \times r} \right\}, \quad W_\delta^p(s) = \ \text{diag}[W_\delta^s(s), I_r] \end{aligned} \tag{16}$$

where $\mu_{\mathbf{\Delta_p}}(\jmath\omega)$ is the structured singular value computed with respect to the new uncertainty structure $\mathbf{\Delta_p}$ ([24]). Again, the value $\mu_{\mathbf{\Delta_p}}(\jmath\omega)$ will be a tight upper

bound on the actual stability margin, depending on how close the weight $w_{\delta i}(s)$ covers the magnitude of the delay uncertainty $\left|e^{-s\delta_i} - 1\right|$ (right plot in Figure 5). As with robust stability, note that to use this analysis tool for controller synthesis is non trivial, because the matrix $T_p(s)$ contains a delayed (infinite dimensional) system $G_o(s)$.

5 MIMO open flow canal example

5.1 Introduction

Let us consider an open flow canal system composed of two pools equipped with two sluice gates and a downstream spillway (see Figure 4). A servomotor is used in each gate to drive the control gate position (u_1 and u_2) and there are two level sensors located downstream of the first (h_1) and second gates (h_2), respectively. The operating range of both gates is limited to the interval [0, 0.9]m. Upstream of the first gate there is a dam of constant level $H = 3.5$ m. The total length of the first pool is $L_1 = 2$ km while in the second $L_2 = 4$ km, with an initial flow q_0 =1 m^3/s, gate discharge coefficient $C_{dg} = 0.6$, a Manning roughness coefficient $n = 0.014$, gate and canal widths of $b = 2.5$ m and $B = 2.5$ m, respectively. The downstream spillway has height $y_s = 0.7$ m, the spillway coefficient is $C_{ds} = 2.66$, and the bottom slope has $I_0 = 5 \times 10^{-4}$.

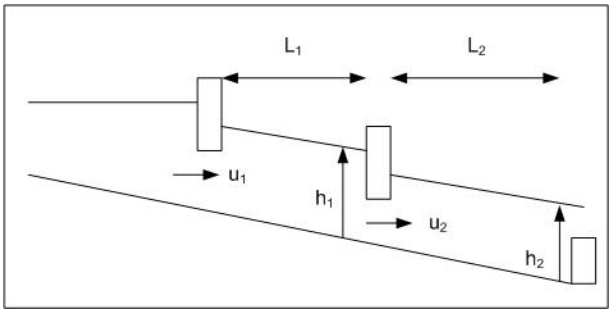

Fig. 4. Two-pool open flow system

This system can be described accurately by the Saint-Venant equations:

$$\frac{\partial q}{\partial x} + \frac{\partial A}{\partial t} = 0 \tag{17}$$

$$\frac{\partial q}{\partial t} + \frac{\partial}{\partial x}\left(\frac{q^2}{A}\right) + gA\frac{\partial y}{\partial x} - gA\left(I_0 - I_f\right) = 0 \tag{18}$$

where $q(x,t)$ is the flow (m^3/s), $A(x,t)$ is the cross-sectional area (m^2), t is the time variable (s), x is the length variable (m), measured in the motion direction, g is the

gravity constant (m/s^2), I_0 is the bottom slope and I_f is the friction slope. This pair of partial-differential equations constitute a nonlinear hyperbolic system, that for an arbitrary geometry lacks of analytical solution. However, such equations are not useful for designing a controller using linear theory as already noticed by [25]. In this reference, a simplified control-oriented model methodology is proposed that allows to describe an n-pool canal system. In this methodology each pool is modelled around a given operating point using the following transfer function matrix

$$\begin{bmatrix} h_i(s) \\ h_{i+1}(s) \end{bmatrix} = \begin{bmatrix} P_{11}(s) & P_{12}(s) \\ P_{21}(s) & P_{22}(s) \end{bmatrix} \begin{bmatrix} q_i(s) \\ q_{i+1}(s) \end{bmatrix} \tag{19}$$

where: $h_i(s)$ and $h_{i+1}(s)$ are the upstream and downstream water levels respectively, and $q_i(s)$ and $q_{i+1}(s)$ are the upstream and downstream flow levels of the pool considered here. $P_{11}(s) = \frac{1}{A_u s}$, $P_{12}(s) = -\frac{1}{A_u s}e^{-\tau_u s}$, $P_{21}(s) = \frac{1}{A_d s}e^{-\tau_d s}$ and $P_{22}(s) = -\frac{1}{A_d s}$ are the transfer functions relating upstream/downstream levels and flows, where A_u and A_d are upstream/downstream backwater areas and τ_u and τ_d are upstream/downstream propagation delays. Additionally, there is a relation between the flow and the opening at each gate that is assumed to be linear:

$$q_i(s) = \alpha_i u_i(s) \tag{20}$$

where α_i is a constant. Finally, taking into account that there is a spillway at the terminal pool that allows to relate the flow with the level in a linear way, the following additional relation should be considered

$$q_n(s) = \beta_n h_n(s) \tag{21}$$

where β_n is a constant.

Applying this modelling methodology to the case of a two pool open flow canal system as the one presented in Figure 4, considering equations (19-21), the following MIMO model is obtained:

$$\begin{bmatrix} h_1(s) \\ h_2(s) \end{bmatrix} = G(s) \begin{bmatrix} u_1(s) \\ u_2(s) \end{bmatrix} \tag{22}$$

where:

$$G(s) = \begin{bmatrix} \frac{k_{11}}{T_{11}s+1}e^{-\tau_{11}s} & \frac{k_{12}}{T_{12}s+1}e^{-\tau_{12}s} \\ \frac{k_{21}}{T_{21}s+1}e^{-\tau_{21}s} & \frac{k_{22}}{T_{22}s+1}e^{-\tau_{22}s} \end{bmatrix} \tag{23}$$

with: $k_{11} = 4.87$, $k_{12} = -4.35$, $k_{21} = 1.2$, $k_{22} = 1.4$, $T_{11} = 30$ min, $T_{12} = 35$ min, $T_{21} = 31.67$ min, $T_{22} = 25$ min, $\tau_{11} \in [5, 9]$ min, $\tau_{12} = 0$ min, $\tau_{21} \in [18, 26]$ min and $\tau_{22} \in [13, 17]$ min.

The delay τ associated to each input/output channel depends on the travelling time of water between input and output. Since the propagation velocity of a flow wave in a canal is equal to the sum of the water velocity and the celerity of the gravity wave, then:

$$\tau = \frac{L}{v + c} \tag{24}$$

where L is the distance between the considered input and output pair. Each delay varies inside its corresponding interval of possible values depending on the input flow that establishes water velocity. This input flow in the proposed application example is controlled through the opening of each gate. In particular, for the proposed two-pool system, if t_1 is the travelling time of the water to cover the first pool of length L_1 and t_2 is the travelling time of the water to cover the second pool of length L_2, the different delays associated to each input/output channel are:

$$\tau_{11} = t_1, \quad \tau_{12} = 0, \quad \tau_{21} = t_1 + t_2, \quad \tau_{22} = t_2 \tag{25}$$

This means that the relation between delays established in Lemma 2.2 holds.

5.2 Internal stability

The rational part of the model is as follows:

$$G_m(s) = \begin{bmatrix} \frac{k_{11}}{T_{11}s+1} & \frac{k_{12}}{T_{12}s+1} \\ \frac{k_{21}}{T_{21}s+1} & \frac{k_{22}}{T_{22}s+1} \end{bmatrix} \tag{26}$$

where all the constants have been defined in the previous subsection. The (left) right coprime factorization is simple, due to the fact that the model is stable. For that reason, a null central controller can be used to apply the Youla parametrization of all stabilizing controllers, as follows:

$$G_m(s) = N_g D_g^{-1} = \tilde{D}_g^{-1}\tilde{N}_g, \qquad N_g = \tilde{N}_g = G_m, \qquad D_g = \tilde{D}_g = I \tag{27}$$

$$K_o(s) = N_k D_k^{-1} = \tilde{D}_k^{-1}\tilde{N}_k, \qquad N_k = \tilde{N}_k = \mathbf{0}, \qquad D_k = \tilde{D}_k = I \tag{28}$$

$$\Longrightarrow \begin{cases} \tilde{N}_g N_k + \tilde{D}_g D_k = I \\ \tilde{N}_k N_g + \tilde{D}_k D_g = I \end{cases} \tag{29}$$

Hence any stabilizing controller, its sensitivity, its complement and the transfer function between reference and control signal are, respectively:

$$K(s) = Q(s)\left[I - G_m(s)Q(s)\right]^{-1} \tag{30}$$

$$S_m(s) = I - G_m(s)Q(s), \qquad T_m(s) = G_m(s)Q(s) \tag{31}$$

$$T_{ur}(s) = K(s)S_m(s) = Q(s) \tag{32}$$

for any stable and proper matrix $Q(s)$. This guarantees nominal internal stability. Further conditions on $Q(s)$ need to be imposed to guarantee robustness against delay uncertainty and performance.

A diagonalization of the closed loop system is always convenient and simplifies the design of $Q(s)$. Note that the rational model, although stable and minimum phase is strictly proper, which can be seen by verifying its inverse is improper, as follows:

$$G_m^{-1}(s) = \frac{1}{d(s)} \cdot \begin{bmatrix} k_{22}(T_{11}s+1)(T_{21}s+1)(T_{12}s+1) & -k_{12}(T_{11}s+1)(T_{22}s+1)(T_{21}s+1) \\ -k_{21}(T_{11}s+1)(T_{22}s+1)(T_{12}s+1 & k_{11}(T_{22}s+1)(T_{21}s+1)(T_{12}s+1) \end{bmatrix} \tag{33}$$

with:

$$\begin{aligned} d(s) = {} & (k_{11}k_{22}T_{21}T_{12} - k_{21}k_{12}T_{11}T_{22})s^2 + (k_{11}k_{22}T_{21} + k_{11}k_{22}T_{12} \\ & - k_{21}k_{12}T_{22} - k_{21}k_{12}T_{11})s + (k_{11}k_{22} - k_{21}k_{12}) \end{aligned}$$

Hence we can achieve complete diagonal sensitivities by using:

$$Q(s) = G_m^{-1}\begin{bmatrix} \tilde{q}_1(s) & 0 \\ 0 & \tilde{q}_2(s) \end{bmatrix} \tag{34}$$

$$T_m(s) = \begin{bmatrix} \tilde{q}_1(s) & 0 \\ 0 & \tilde{q}_2(s) \end{bmatrix}, \quad S_m(s) = \begin{bmatrix} 1-\tilde{q}_1(s) & 0 \\ 0 & 1-\tilde{q}_2(s) \end{bmatrix} \tag{35}$$

Here both rational SISO transfer functions $\tilde{q}_1(s)$ and $\tilde{q}_2(s)$ need to be stable and *strictly* proper, to guarantee stability and properness of $Q(s)$. They should be selected so that robustness against time delay uncertainty is guaranteed and a reasonable performance is obtained, as will be seen in next subsection. In addition, channel decoupling is achieved, at least in the nominal case.

5.3 Robust Stability

Based on the results of subsection 3.1, in particular Lemma 3.1, the global dynamic uncertainty should be covered by a weight based on the condition number of $G_m(s)$. In this case, this is extremely conservative ($7 \geq 2\kappa\left[G_m(\jmath\omega)\right] \geq 6$) and instead we cover the (parametric) delay uncertainty with global dynamic uncertainty, using equation (D.1). In this case, the nominal delays and their uncertainty intervals are as follows (in minutes):

$$D_\ell(s) = \begin{bmatrix} 1 & 0 \\ 0 & e^{-s(15\pm 2)} \end{bmatrix}, \; D_r(s) = \begin{bmatrix} e^{-s(7\pm 2)} & 0 \\ 0 & 1 \end{bmatrix} \tag{36}$$

The delay uncertainties intervals are gridded and the magnitude curves for equation (D.1) at all points are shown in the left plot of Figure 5. The global dynamic uncertainty weight should therefore cover the delay parametric uncertainty represented by all these curves, as shown in the same figure. The resulting weight is in this case:

$$W_\delta(s) = \frac{k_\delta \; s}{s + p_\delta} I_{2\times 2} \tag{37}$$

where $k_\delta = 3.5$ and $p_\delta = 2 \cdot 10^{-3}$. This coverage is less conservative than the one obtained in Lemma 3.1, based on the condition number of $G_m(s)$. In addition, for analysis purposes we will also apply the condition based on the coverage of structured uncertainty of section 3.2.

To achieve robust stability, we can further restrict the free parameters [$\tilde{q}_1(s)$,$\tilde{q}_2(s)$] as follows: $\tilde{q}_i(s) = w_{\delta_i}^{-1} q_i(s)$, $i = 1, 2$. The new parameters should be stable, *strictly* proper and norm bounded by one, i.e. $|q_i(\jmath\omega)| < 1, \forall\omega, \; i = 1, 2$. Hence we achieve the equivalent robust stability condition:

$$\left\|W_\delta(s) T_m(s)\right\|_\infty = \left\| \begin{bmatrix} q_1(s) & 0 \\ 0 & q_2(s) \end{bmatrix} \right\|_\infty = \begin{cases} \max\left\{|q_1(s)|, |q_2(s)|\right\} < 1, \\ \forall s = \jmath\omega \end{cases} \tag{38}$$

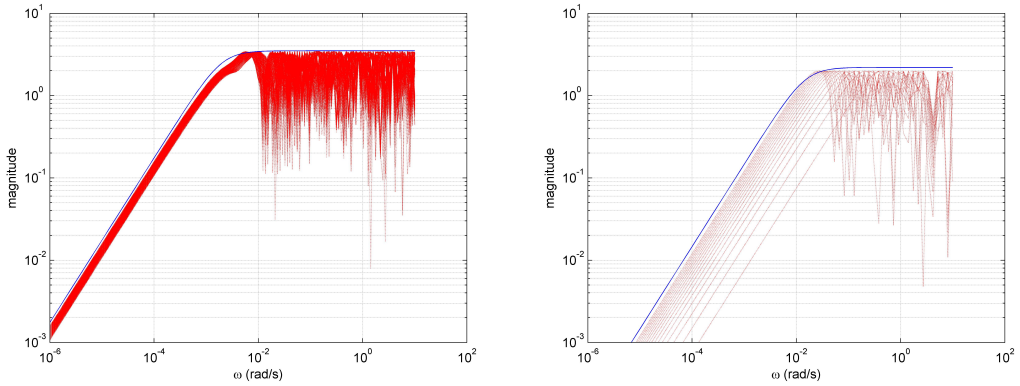

Fig. 5. Global $W_\delta(s)$ (full-left) and structured $w_{\delta i}(s)$ (full-right) dynamic uncertainty weights covering the delay parametric uncertainty.

5.4 Robust Performance

The free parameter from previous subsection which already guaranteed robust stability under (global) dynamic uncertainty, and the corresponding sensitivities and controller are the following:

$$Q(s) = [W_\delta(s) G_m(s)]^{-1} \begin{bmatrix} q_1(s) & 0 \\ 0 & q_2(s) \end{bmatrix} \tag{39}$$

$$T_m(s) = G_m(s) Q(s) = [W_\delta(s)]^{-1} \begin{bmatrix} q_1(s) & 0 \\ 0 & q_2(s) \end{bmatrix}, \; S_m(s) = I - T_m(s) \tag{40}$$

with $q_1(s)$ and $q_2(s)$ stable, *strictly* proper and norm bounded by one, i.e. $|q_i(\jmath\omega)| < 1, \forall\omega, \; i = 1, 2$.

Here we solve the robust tracking error (**TE**) problem by an appropriate selection of these parameters. Hence by replacing the previous expressions in equation (14), the following robust performance sufficient condition is obtained:

$$\max\left(|q_1(s)|, |q_2(s)|\right) + \bar{\sigma}\left\{ W_e(s) \left(I - W_\delta^{-1}(s) \begin{bmatrix} q_1(s) & 0 \\ 0 & q_2(s) \end{bmatrix} \right) \right\} \leq 1$$

for all $s = \jmath\omega$. Note that the second term restricts even more the robust stability condition represented by the first term. In the simplified case in which the weights are diagonal, i.e. $W_e(s) = \text{diag}[w_{e1}(s), w_{e2}(s)]$, $W_\delta(s) = \text{diag}[w_{\delta 1}(s), w_{\delta 2}(s)]$,

the previous condition results:

$$\max\{|q_1(s)|, |q_2(s)|\} + \max\left\{|w_{e1}(s)|\left|1 - \frac{q_1}{w_{\delta 1}}(s)\right|, |w_{e2}(s)|\left|1 - \frac{q_2}{w_{\delta 2}}(s)\right|\right\} \leq 1$$

for all $s = \jmath\omega$.

In the previous condition we allow two different parameters to be selected for the design: q_1 and q_2. If we further simplify both robustness and performance weights to have the form $w_x(s)I_{n\times n}$, this extra freedom does not add any benefit. Therefore, in this case we may as well select $Q(s)$ with both diagonal element equal, i.e. $q_1 = q_2 = q(s)$. Hence the previous robust performance condition reduces to:

$$|q(s)| + |w_e(s)|\left|1 - \frac{q(s)}{w_\delta}(s)\right| \leq 1, \ \forall s = \jmath\omega \tag{41}$$

Here we have selected a simple (low order) performance weight, so that the order of the controller is kept low. Furthermore, this weight $W_e(s)$ forces the closed loop system to reject constant and low frequency disturbances as follows:

$$W_e(s) = \frac{s + z_e}{2\ s} I_{2\times 2} \tag{42}$$

We have selected $z_e = 0.5 \cdot 10^{-4}$ that maximizes performance while maintaining control signals (u_1 and u_2) inside the operating ranges.

In order to satisfy the robust performance condition (41) and yet not to increase the order of the controller, we select the simplest parameter $q(s)$. From the observation of equation (41), it is clear that in order to have the second term below one, $q(s)$ should cancel the pole at the origin of $W_e(s)$ and $W_\delta^{-1}(s)$. This cannot be achieved with a constant $q(s)$, but instead needs at least a pole and a zero, as follows:

$$q(s) = \frac{q_o s}{(s + p_q)}$$

The zero in $s = 0$ cancels the one in $W_\delta(s)$, and to cancel the pole in $s = 0$ of $W_e(s)$, the following conditions should be met: $q_o/p_q = k_\delta/p_\delta$. The values in this case are as follows $p_q = 4 \cdot 10^{-4}$ and $q_o = 0.57$. Finally, due to the fact that $q(s)$ should be strictly proper, we add an extra pole which will be used as an extra degree of freedom in designing the controller, hence:

$$q(s) = \frac{q_o s}{(s + p_q)(\tau s + 1)} \tag{43}$$

By replacing the free parameter in equation (30), and using equation (33), we obtain the following proper controller:

$$K(s) = G_m^{-1}(s)\frac{q(s)}{w_\delta - q(s)} = G_m^{-1}(s)\frac{q_o(s+p_\delta)}{s[sk_\delta\tau + k_\delta(\tau p_q + 1) - q_o]} \tag{44}$$

The previous design of $K(s)$ has considered the case of global dynamic uncertainty, represented by weight $W_\delta(s)$. In this case, the gain in (44) is chosen as $q_o = 0.57$, and the resulting performance and robustness conditions are presented in Figure 6.

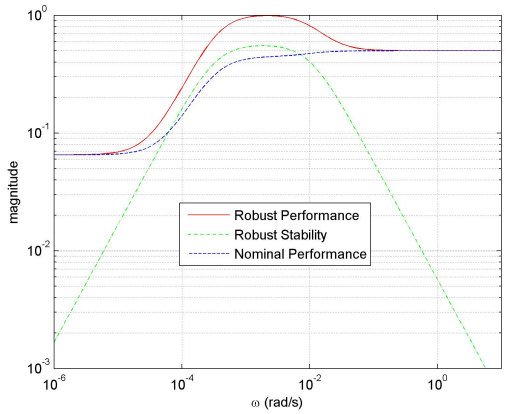

Fig. 6. Robust stability and nominal & robust performance conditions for global uncertainty coverage.

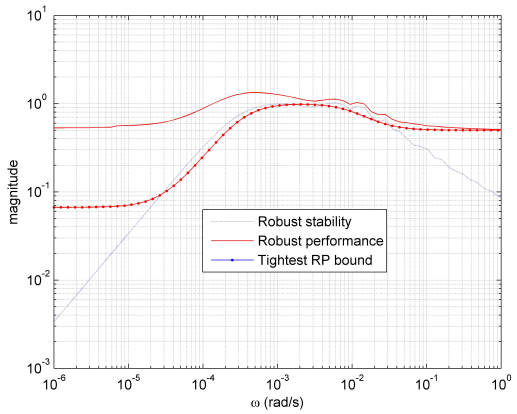

Fig. 7. Robust stability and performance conditions for structured uncertainty coverage.

Furthermore, for analysis purposes both upper bounds on the robust stability and performance conditions based on the structured uncertainty results of sections 3.2 and 4.3, are verified. Here, the (structured) uncertainty at each delay is covered by the weight $w_\delta(s) = \frac{2.2\ s}{s+0.015}$ shown in the right side of figure 5, for both $i = 1, 2$, i.e. $W_\delta^s(s) = w_\delta(s) I_{2\times 2}$. Note that this coverage limits the performance less than the

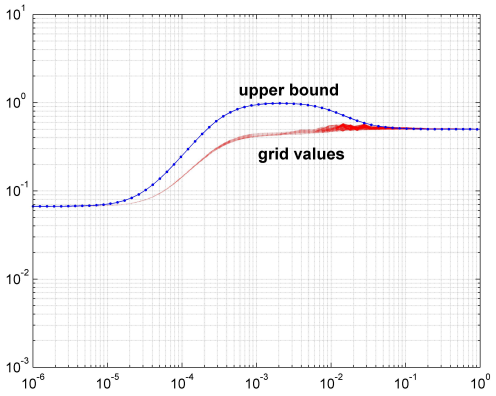

Fig. 8. Comparison of actual and sufficient robust performance condition.

global one at the left of the same figure, due to the fact that the 0 dB crossing is at a higher frequency. Finally, we obtain the tightest upper bound on robust performance by computing the minimum at each frequency of the upper bounds in equations (41) and (16). This has been illustrated in figure 7, where the (sufficient) robust stability and performance conditions based on the results of section 4.3, as well as the combined lower bound have been represented. Note that both upper bounds on robust performance (41) and (16), contribute to the minimum (dash-dot line) at different frequency ranges.

In addition we compare this tighter bound with the actual value of robust performance based on the uncertainty computed by a gridding method, to measure the degree of conservativeness. Recall that we have mentioned the fact that the correct measure to compute robust stability or robust performance with structured uncertainty should be calculated via the structured singular value $\mu_{\mathbf{\Delta_s}}$ or $\mu_{\mathbf{\Delta_p}}$ based on $\mathbf{\Delta_s}$ or $\mathbf{\Delta_p}$ structures of pure MIMO delay uncertainty, respectively. These cannot be computed exactly with existing algorithms, therefore we have computed the robust performance condition with structured uncertainty, by gridding the uncertain δ_i's for the delays, in the nominal performance condition (10). Here, $T_{er}(s)$ in equation (12) has been replaced by the actual (uncertain) matrix, which results in the following (structured) robust performance condition:

$$\left\| W_e S_m \left[I + (G - G_o) Q \right]^{-1} \right\|_\infty < 1 \tag{45}$$

for all $|\delta| < 2$ minutes. The comparative robust performance conditions are illustrated in figure 8. From this figure it could be concluded that possibly a higher gain could have been used in the design, but other practical issues prevent this in the final design. Also it is important to emphasize that there is no optimal synthesis procedure yet to compute the best controller under this structured type of delay un-

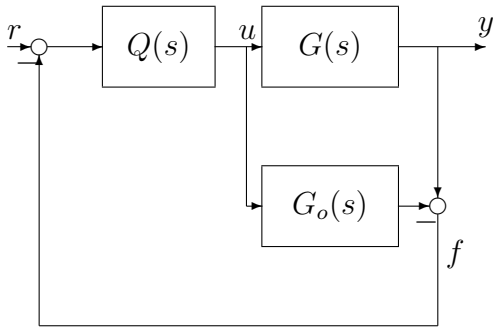

Fig. 9. Smith Predictor implementation (as in IMC).

certainty. The only procedure that could be applied but only for the nominal plant, would be the one in [19].

5.5 Low and High fidelity Simulations

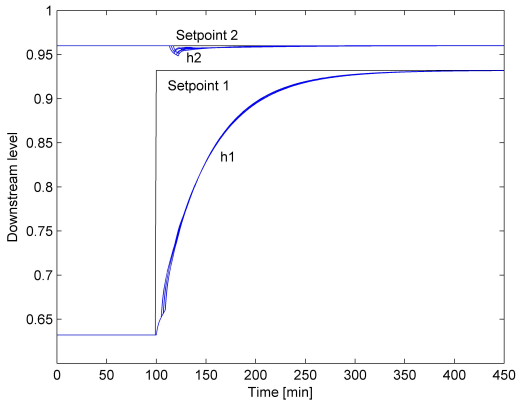

Fig. 10. Downstream levels h_1 and h_2 in case of a change in the opening set-point of the upstream gate u_1.

In order to validate the design, the controller is initially tested against the simulated plant given by equation (23). From figure 1, by replacing $K(s)$ as a function of $Q(s)$ as in (30), we obtain figure 9, which is a much simpler implementation, as used in IMC ([17]). Multiple responses to a step change in the opening set-point of the upstream gate u_1, using a grid of delays inside the admissible interval are generated. The set-point for level h_2 is kept constant at 0.96 meters, to verify decoupling among channels, considered in the design phase. In Figure 10, the time evolution of downstream levels h_1 and h_2 are presented. From these figures, it can be observed that the tracking error of the downstream level h_1 goes to zero, due to the controller integrator. Furthermore, the effect of (energy) bounded perturbations

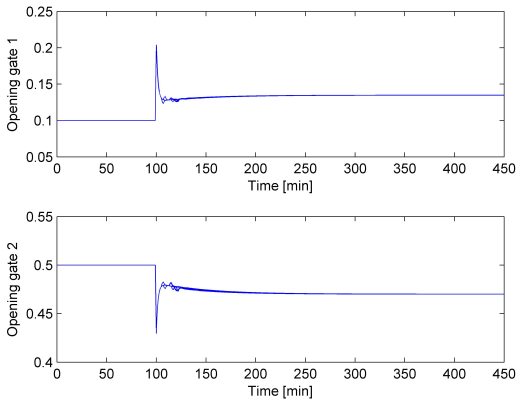

Fig. 11. Both actuator gate responses in case of a change in the opening set-point of the upstream gate u_1.

is also attenuated, mainly in the frequencies indicated by the design weight $W_e(s)$. A perfect decoupling is achieved in the nominal case, but not in general due to the uncertainty. Nevertheless, a good decoupling of the effect on downstream level h_2 can be observed for the set of curves. The limitation of control action has been considered in the design, also through the performance weight $W_e(s)$. In figure 11, the associated gate opening control signals u_1 and u_2 are presented. Both control signals are well inside the interval of admissible values $[0, 0.9]$, as expected.

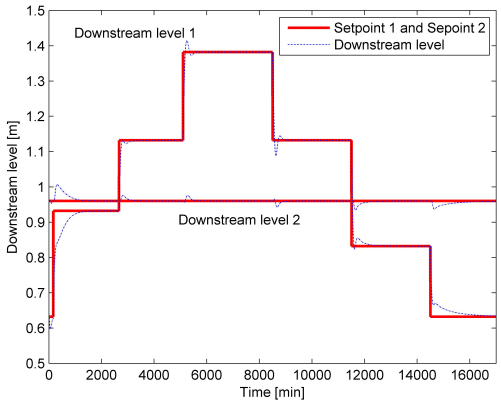

Fig. 12. Downstream levels h_1 and h_2 for a set-point step.

The next step is to apply the previous controller to a high fidelity simulator that reproduces the "actual" canal behavior. This simulator has been developed and validated by the group *Modelling and Control of Hydraulic Systems* at the UPC. It is based on solving numerically Saint-Venant's equations (see equations (18)).

A scenario based on a sequence of steps that covers the whole operating range of the two-pool canal system is applied as a set-point for level h_1. The set-point for

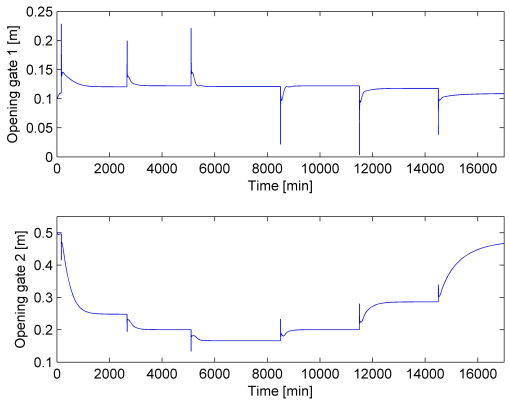

Fig. 13. Gate opening control signals u_1 and u_2 for set-point step.

level h_2 is again kept constant an equal to 0.96 meters, to test decoupling. The set-point changes in h_1 are followed without steady state error and with good performance. Stability robustness is also good, in spite of the delay variations in this scenario, which also excites the nonlinear behavior of the plant. In Figure 12, the time evolution of downstream levels h_1 and h_2 is presented. Again, it can be observed that the results in terms of performance and robustness are similar to the previous ones. Moreover, the decoupling effect on the downstream level h_2 is again very acceptable. In Figure 13, the associated gate opening control signals u_1 and u_2 are presented. The results of previous simulations are validated, provided the control signals are inside the admissible interval $[0, 0.9]$.

6 Comparative Example

A second example based on the known binary distillation column presented in [26] is proposed, and a brief analysis with our method has been made for comparison. The transfer function matrix corresponding to this system is the following:

$$G(s) = \begin{bmatrix} \frac{12.8}{16.7s+1}e^{-s} & \frac{-18.9}{21s+1}e^{-3s} \\ \frac{6.6}{10.9s+1}e^{-7s} & \frac{-19.4}{14.4s+1}e^{-3s} \end{bmatrix} \tag{46}$$

This example has also been used in [6,12,13] in the context of MIMO Smith Predictor design methods. To fit the conditions in equation (5) from Lemma 2.2, the nominal values have been re-defined and included in the following uncertainty intervals so that all values of the model are considered (as commented in footnote 3):

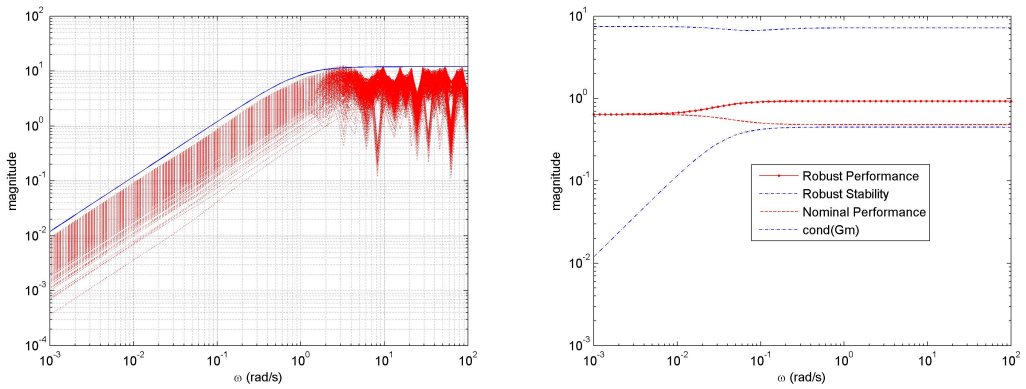

Fig. 14. (left) Global dynamic uncertainty weight $W_\delta(s)$ (full) covering the delay parametric uncertainty and (right) robust stability and performance analysis.

Nominal values:

$$\tau_{11} = 2,\ \tau_{21} = 6,\ \tau_{12} = 1,\ \tau_{22} = 5 \implies \tau_{11} - \tau_{21} = \tau_{12} - \tau_{22} \tag{47}$$

Uncertainty intervals:

$$\delta_{11} \in [-1, 0],\ \delta_{21} \in [0, 1],\ \delta_{12} \in [0, 2],\ \delta_{22} \in [-2, 0] \tag{48}$$

A design similar to the one used in the previous example produced a robustly stable controller with robust performance and stability guarantees. The left plot in figure 14 represents the delay interval uncertainty coverage by a global dynamic uncertainty weight, using equation (D.1). Here, the delay uncertainty intervals are gridded and the magnitude curves for equation (D.1) at all points are shown in the same plot. The global dynamic uncertainty weight covers the delay parametric one, resulting in the following:

$$W_\delta(s) = \frac{12\ s}{s+1} I_{2\times 2} \tag{49}$$

The performance weight $W_e(s)$ should force the closed loop system to reject constant and low frequency disturbances and has been selected as:

$$W_e(s) = \frac{s + 0.05}{2\ s} I_{2\times 2} \tag{50}$$

In order to satisfy the robust performance condition (41) and yet not to increase the order of the controller, a preliminary selection of $q(s)$ is:

$$\tilde{q}(s) = \frac{q_o s}{(s + p_q)}$$

In addition, to cancel the pole in $s = 0$ of $W_e(s)$, the following condition should be met: $q_o/p_q = 12$, therefore the values are selected as: $p_q = 0.0375$ and $q_0 = 0.45$. Finally to make $q(s)$ strictly proper, an extra pole is added:

$$q(s) = \frac{q_o s}{(s + p_q)(10^{-3}s + 1)} \tag{51}$$

The right plot illustrates the nominal and robust performance and robust stability guarantees (all below 1). In that same figure we see that the condition number is, also in this example, a conservative measure of global robustness. As noted from (47) and (48), here the uncertainty in all delays is much larger than the 15% considered, only for diagonal delays, in [12]. Beyond that point in that example, the system went unstable. Furthermore in [12] there was no quantification of the robustness margin, only a trial and error attempt to test the controller.

Concerning the achievable decoupling regulation, figure 15 presents a set-point step change in each channel separately. It shows a very good decoupling for the whole set of plants included in the uncertainty intervals. Moreover, it can be noticed that in spite of the delay uncertainty considered, the stability is preserved for the whole set of models. Finally, figure 16 shows that the previous step responses are obtained using reasonable values for the control inputs.

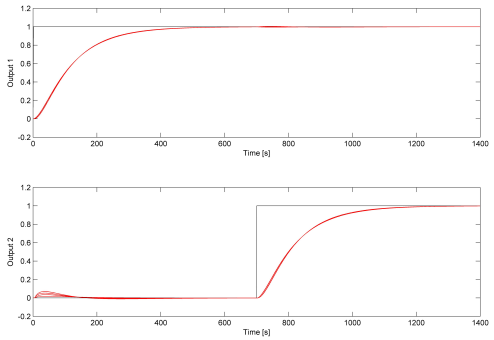

Fig. 15. Outputs y_1 and y_2 in case of a change in both set-points.

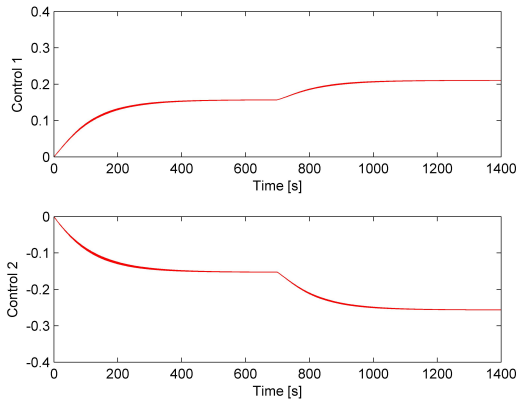

Fig. 16. Controller outputs u_1 and u_2 in case of a change in both set-points.

7 Conclusions

This paper presented an extension of the classical Smith Predictor to MIMO systems with multiple uncertain delays. A set of necessary and sufficient conditions under which a model can be separated into diagonal left and right pure delays and a rational matrix is presented. Surprisingly, these conditions are satisfied by multiple pool open flow canal systems. Stability, robustness and performance analysis conditions are presented for these class of plants in two cases: global dynamic and structured parametric uncertainty. To date, there is no exact way of computing both structured robust stability and performance conditions. Hence, two upper bounds are computed, based on covering the delay uncertainty in two different ways, globally and individually. To test these results, a controller is designed for a two-pool canal system, and its performance and robustness are evaluated. The conservativeness of the robust performance measures under structured delay uncertainty is computed. Further research needs to be done both, in computing the exact (structured) robust stability and performance margins, and in producing an optimal design procedure for this particular uncertain class of models.

References

[1] O. J. M. Smith, Closer control of loops with dead time, Chemical Engineering Progress 53 (1957) 217–219.

[2] Z. J. Palmor, The Control Handbook, CRC and IEEE Press, 1996, Ch. Time Delay Compensation, pp. 224–237.

[3] G. Alevisakis, D. Seborg, An extension of the Smith predictor method to multivariable

linear systems containing time delays, International Journal of Control 17 (1973) 541–551.

[4] C. Moore, C. Smith, P. Murril, Improved algorithm for DDC, Instrumentation Control Systems 43 (1).

[5] P. Frank, Entwurf von Regelkreisen mit vorgeschriebenem Verhalten (Design of Control loops with prescribed behavior), G.Braun, Karlsruhe, 1974.

[6] B. Ogunnaike, W. Ray, Multivariable controller design for linear systems having multiple time delays, AIChE Journal 25 (1979) 1043–1057.

[7] Z. Palmor, Y. Halevi, On the design and properties of multivariable dead time compensators, Automatica 19 (1983) 255–264.

[8] A. Bhaya, C. Desoer, Controlling plants with delay, International Journal of Control (1985) 813–830.

[9] D. H. Owens, Robust stability of Smith predictor controllers for time delay systems, Proceedings of IEE, Part D 129 (1982) 298–304.

[10] C. Garcia, M. Morari, Internal Model Control. 2. Design Procedure for Multivariable Systems, Eng. Chem. Process Des. Dev. (6) (1985) 472–484.

[11] N. F. Jerome, W. H. Ray, High-performance multivariable control strategies for systems having time delays, AIChE Journal 32 (6) (1986) 914–931.

[12] Q. G. Wang, Y. Zhang, M. S. Chiu, Decoupling internal model control for multivariable systems with multiple time delays, Chemical Engineering Science 57 (2002) 115–124.

[13] Q. Wang, B. Zou, Y. Zhang, Decoupling Smith predictor design for multivariable systems with multiple time delays, Chemical Engineering Research and Design Transactions, part A 78 (4) (2000) 565–572.

[14] T. Liu, W. Zhang, F. Gao, Analytical decoupling control strategy using a unity feedback control structure for MIMO processes with time delays, Journal of Process Control(In Press, available online 17 October 2006).

[15] J. M. Maciejowski, Robustness of multivariable Smith predictors, Journal of Process Control 4 (1) (1994) 29–32.

[16] W. Feng, On practical stability of linear multivariable feedback systems with time delays,, Automatica 27 (1991) 389–394.

[17] M. Morari, E. Zafirou, Robust Process Control, Prentice Hall, NJ, 1989.

[18] Z. Palmor, Stability properties of Smith dead-time compensator controllers, International Journal of Control 53 (1980) 937–949.

[19] G. Meinsma, L. Mirkin, $\mathcal{H}_\infty$ control of systems with multiple I/O delays via decomposition to adobe problems, IEEE Transactions on Automatic Control 50 (2) (2005) 199–211.

[20] R. S. Sánchez Peña, M. Sznaier, Robust Systems Theory and Applications, John Wiley & Sons, Inc., 1998.

[21] X. Litrico, Robust IMC flow control of SIMO dam-river open channel systems, IEEE Transactions on Control Systems Technology 10 (3) (2002) 432–437.

[22] J. Hlava, Decoupling anisochronic internal model controllers for MIMO systems with state delays, in: 5th workshop on Electronics, Control, Modelling, Measurement and Signals, Toulouse - France, 2001, pp. 195–201.

[23] S. Skogestad, I. Postlethwaite, Multivariable Feedback Control: Analysis and Design, John Wiley and Sons, 1996.

[24] J. C. Doyle, Analysis of feedback systems with structured uncertainty, IEE Proceedings: part D 129 (6) (1982) 242–250.

[25] X. Litrico, V. Fromion, Simplified modeling of irrigation canals for controller design, Journal of Irrigation and Drainage Engineering 130 (5) (2004) 373–383.

[26] R. Wood, M. Berry, Terminal composition control of a binary distillation column, Chemical Engineering Science 28 (1973) 1707–1717.

A Proof of Lemma 2.1:

The rank r of H is at most $n + m - 1$, because its null space has at least rank one:

$$H \begin{bmatrix} \mathbf{1}_n \\ -\mathbf{1}_m \end{bmatrix} = \mathbf{0}_{nm} \tag{A.1}$$

Furthermore, it is a fact that equation (4) has at least one solution if $n \cdot m \leq r \leq n + m - 1 \Longleftrightarrow n(m-1) \leq (m-1)$, which in turn is equivalent to:

$$\begin{cases} n = 1, \quad \forall m \geq 1 \\ m = 1, \quad \forall n \geq 1 \end{cases} \tag{A.2}$$

therefore, only applicable to SIMO or MISO models. The case of diagonal systems is similar to SISO systems, and does not need a proof.

□

B Proof of Lemma 2.2:

Necessary Consider in equation (4), the q-th and k-th (block) rows:

$$\begin{bmatrix} \tau_{1q} \\ \vdots \\ \tau_{nq} \end{bmatrix} = \begin{bmatrix} \tau_1^\ell \\ \vdots \\ \tau_n^\ell \end{bmatrix} + \begin{bmatrix} \tau_q^r \\ \vdots \\ \tau_q^r \end{bmatrix}, \qquad \begin{bmatrix} \tau_{1k} \\ \vdots \\ \tau_{nk} \end{bmatrix} = \begin{bmatrix} \tau_1^\ell \\ \vdots \\ \tau_n^\ell \end{bmatrix} + \begin{bmatrix} \tau_k^r \\ \vdots \\ \tau_k^r \end{bmatrix} \tag{B.1}$$

Hence, subtracting the i-th and j-th rows in both equations we obtain:

$$\tau_{iq} - \tau_{jq} = \tau_q^\ell - \tau_k^\ell = \tau_{ik} - \tau_{jk}$$

This procedure can be applied to all $i, j = 1, \ldots, n$ and all $q, k = 1, \ldots, m$ and provides necessary conditions on the system's delays $\{\tau_{ik},\ i = 1, \ldots, n;\ k = 1, \ldots, m\}$ for a solution to exist.

Sufficient Extract the first row, the $n+1$-th, $2n+1$-th rows and so on, from equation (4), up to row $(m-1)n+1$. The resulting equation, as well as the first equation in (B.1) for $q = 1$, are as follows:

$$\begin{bmatrix} \tau_{11} \\ \vdots \\ \tau_{1m} \end{bmatrix} = \begin{bmatrix} \tau_1^r \\ \vdots \\ \tau_m^r \end{bmatrix} + \tau_1^\ell \mathbf{1}_m, \qquad \begin{bmatrix} \tau_{11} \\ \vdots \\ \tau_{n1} \end{bmatrix} = \begin{bmatrix} \tau_1^\ell \\ \vdots \\ \tau_n^\ell \end{bmatrix} + \tau_1^r \mathbf{1}_n \tag{B.2}$$

which represents $n+m$ linear equations with $n+m$ unknowns ($\tau_i^\ell, \tau_k^r, i = 1, \ldots, n;\ k = 1, \ldots, m\}$). Note also that the first equation in both sets is the same, i.e. $\tau_{11} = \tau_1^\ell + \tau_1^r$, therefore the kernel has at least dimension one and this set of equations has an infinite number of solutions, in accordance with the fact proved in Lemma 2.1 that H has at most rank $n + m - 1$.

□

C Proof of Corollary 2.1:

Without loss of generality we will prove the lower triangular case, the upper case being proved in a similar way. Here $n = m$ and $\tau_{ij} \neq 0$ for $i \geq j$, with $\tau_{ij} = 0$ otherwise. The linear equation in (4) reduces to:

$$\begin{bmatrix} \tau_{11} \\ \vdots \\ \tau_{n1} \\ \tau_{22} \\ \vdots \\ \tau_{n2} \\ \vdots \\ \tau_{(n-1)(n-1)} \\ \tau_{n(n-1)} \\ \tau_{nn} \end{bmatrix} = \begin{bmatrix} I_n & & \mathbf{1}_n & \mathbf{0}_{n\times(n-1)} & \\ \mathbf{0}_{n-1} & I_{n-1} & \mathbf{0}_{n-1} & \mathbf{1}_{n-1} & \mathbf{0}_{n-1\times(n-2)} \\ \vdots & \vdots & \vdots & \vdots & \vdots \\ \mathbf{0}_{2\times(n-2)} & I_2 & \mathbf{0}_{2\times(n-1)} & \mathbf{1}_2 & \mathbf{0}_2 \\ \mathbf{0}_{1\times(n-1)} & 1 & \mathbf{0}_{1\times(n-1)} & & 1 \end{bmatrix} \begin{bmatrix} \tau_1^\ell \\ \vdots \\ \tau_n^\ell \\ \tau_1^r \\ \vdots \\ \tau_n^r \end{bmatrix} \triangleq H_\triangleright \tau$$

with $H_\triangleright \in \mathbb{R}^{\ell\times 2n}$, and $\ell = \frac{n(n+1)}{2}$. As in the previous more general case (Lemma 2.1),

$$H_\triangleright \begin{bmatrix} \mathbf{1}_n \\ -\mathbf{1}_n \end{bmatrix} = \mathbf{0}_\ell$$

Therefore the rank $r \leq 2n-1$, and there is a solution if and only if:

$$\begin{aligned} & \ell = \frac{n(n+1)}{2} \leq 2n-1 \\ \iff \quad & n^2 - 3n + 2 \leq 0 \\ \iff \quad & 1 \leq n \leq 2 \end{aligned}$$

This applies only to integers $n \in \{1, 2\}$ and proves the first part of the corollary. For the general case of lower triangular systems, equations (5) apply, now taking into account that only τ_{ik} for $i \geq k$ have nonzero values and are zero otherwise, hence less conditions need to be satisfied.

□

D Proof of Lemma 3.1:

Both uncertain matrices in equation (7) are inner factors (*modulo* $\sqrt{2}$), i.e.

$$U(s) \stackrel{\triangle}{=} \frac{1}{\sqrt{2}} \begin{bmatrix} \Delta_{\ell(r)}(s) & \pm I \end{bmatrix} \Longrightarrow U(s)U^*(s) = I$$

applying the definitions of Δ_ℓ and Δ_r and the property that complex exponentials have unit magnitude. Therefore, to cover equation (7) with the set $\mathcal{G}(s)$ in (8), we obtain:

$$\begin{aligned} \bar{\sigma}\left[W_\delta(\jmath\omega)\right] &\geq 2\frac{\bar{\sigma}\left[G_o(\jmath\omega)\right]}{\underline{\sigma}\left[G_m(\jmath\omega)\right]} = 2\frac{\bar{\sigma}\left[G_m(\jmath\omega)\right]}{\underline{\sigma}\left[G_m(\jmath\omega)\right]} = 2\kappa\left[G_m(\jmath\omega)\right] \\ \Longrightarrow \bar{\sigma}\left[\Delta W_\delta(\jmath\omega)\right] &\geq \bar{\sigma}\left\{ \begin{bmatrix} \Delta_\ell(\jmath\omega) & -I \end{bmatrix} G_o(\jmath\omega) \begin{bmatrix} \Delta_r(\jmath\omega) \\ I \end{bmatrix} G_m^{-1}(\jmath\omega) \right\} \end{aligned} \tag{D.1}$$

for all $\bar{\sigma}(\Delta) < 1$. We have used the fact that $\bar{\sigma}\left[G_o(\jmath\omega)\right] = \bar{\sigma}\left[\bar{D}_\ell(\jmath\omega)G_m(\jmath\omega)\bar{D}_r(\jmath\omega)\right] = \bar{\sigma}\left[G_m(\jmath\omega)\right]$, based on the definitions of $\bar{D}_\ell$ and $\bar{D}_r$.

□